Proof of the Resonant Acceleration Mechanism for Fast Electrons in Gaseous Laser Targets*

Paul Kolodner and Eli Yablonovitch
Gordon McKay Laboratory, Harvard University, Cambridge, Massachusetts 02138
(Received 24 August 1976)

We report the observation of fast-electron emission (10–20 keV) from gaseous targets irradiated by a CO_2 laser pulse. The electrons are emitted in a direction 30° away from the electric vector, but in the plane of optical polarization. This is the first direct experimental observation of the resonant absorption effect, which has been proposed as being responsible for the efficient laser energy deposition in a plasma. In contrast, the parametric decay instability is not consistent with the observations.

The mechanism of light absorption remains one of the crucial unanswered questions in laser-plasma interaction. It is generally agreed that the energy is abosrbed in the narrow critical layer where the plasma frequency ω_p equals the laser frequency ω. Among the suggested mechanisms are the parametric decay instability[1] (PDI) and the resonant absorption (RA) effect.[2] In this Letter we show that, for gaseous targets at least, resonant absorption is the dominant mechanism.

In studying basic physical phenomena, gaseous targets offer some definite advantages over solid targets. For example, it has been found[3] that the plasma density is actually equal to the density of the neutral gas in which it is formed. Thus the plasma density can be controlled by simply varying the gas pressure of the target. To be specific, 150-Torr hydrogen gas, at room temperature, has a density of 10^{19} atoms/cm^3, which is the critical density for the CO_2 laser frequency.

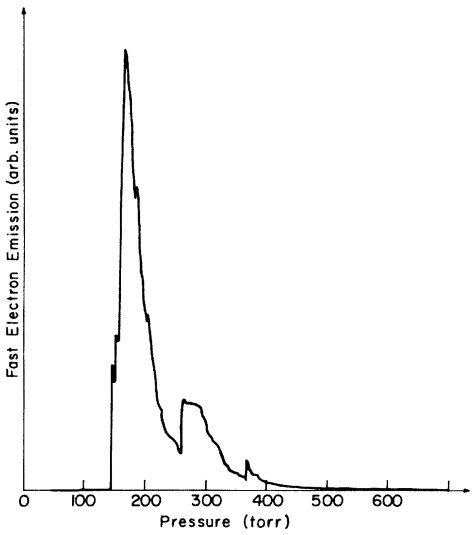

FIG. 1. Electron emission vs pressure for H_2 gas. Notice the sudden onset of fast-electron emission at 150 Torr. At that pressure the gas density is 10^{19} atoms/cm^3, the critical plasma density for the CO_2 laser. The output from a silicon radiation detector was averaged in a boxcar amplifier to produce this curve.

In Fig. 1 is a plot of the fast-electron emission versus pressure in a hydrogen gas target. Notice the sudden onset at 150 Torr.

It is important to ask, under what physical circumstance may we expect to predict the plasma density in this simple way? We need to know the degree of ionization of the gas and its density. At the laser intensity of $10^{13}-10^{14}$ W/cm^2, the electron energy[4] is sufficient to ensure 100% ionization of the H_2 gas in a time much less than the pulse duration. Also at these intensities, the ionization front propagates[5] into the neutral gas at a speed $\sim 10^8$ cm/sec, greatly in excess of the ion sound speed. Therefore the plasma rarefaction wave is unable to keep up with the ionization front and the gas density is unchanged upon ionization.

The sudden onset of fast-electron emission at 150-Torr H_2 gas (Fig. 1) indicates that the acceleration mechanism depends on the presence of a critical density of electrons. Both the PDI and the RA mechanism rely on the condition $\omega_p \sim \omega$, and both predict the acceleration of some electrons to high energy. To distinguish between these two mechanisms we must look at them in closer detail.[6]

In the PDI the light wave drives an instability[1] of electron plasma oscillations and ion sound waves propagating in the direction of the electric vector. As the plasma waves undergo Landau damping, they generate a superthermal tail of high-energy electrons moving parallel and antiparallel to the electric vector of the pump wave.

In the RA mechanism,[2] the light wave is assumed obliquely incident on a varying plasma density profile. The light field penetrates the evanescent region and the electric vector component which is parallel to the plasma density gradient drives resonant oscillations at the critical layer. The plasma wave amplitude builds up until "wave breaking" or "electron overtaking" occurs.[7] Then

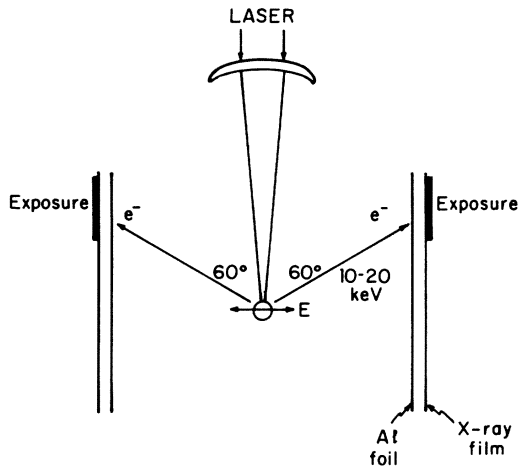

FIG. 2. Geometry of the experiment. The laser is focused to produce a plasma in hydrogen gas. Fast electrons were emitted in the plane of the page, in the two directions shown. This proves that resonant absorption rather than the parametric decay instability is responsible for the acceleration.

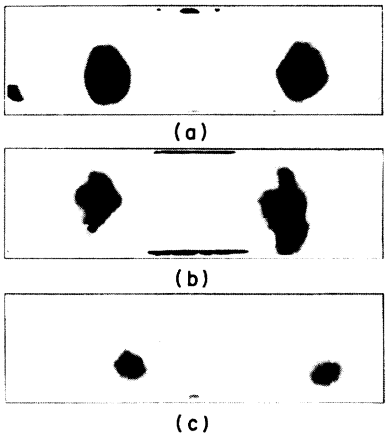

FIG. 3. The x-ray film was bent into the shape of a cylinder, co-axial with the laser beam, and exposed to the fast electrons. (a),(b) two typical shots. Notice the angular substructure in (b). (c) The plane of polarization rotated 45°. The two spots are correspondingly shifted.

the oscillatory energy of the electrons is converted to directed kinetic energy and they are ejected down (but not up) the plasma density gradient. The effect is maximized at some oblique angle of incidence θ, whose exact value depends on the density-profile scale length L.

The basic experimental result of this Letter is shown in Fig. 2: (i) The electrons are emitted at an oblique angle with respect to the electric vector, in the plane formed by the electric vector and the propagation vector. (ii) Furthermore, there are no electrons emitted antiparallel to either of the two directions shown. This is overwhelming evidence in favor of the RA mechanism.

The laser source was a Tachisto CO_2 single-mode oscillator, followed by an optical free-induction-decay[8] (OFID) pulse shaper and a Lumonics 103 amplifier. This system is more fully described by Kwok and Yablonovitch.[9] The output is a diffraction-limited pulse of 0.15-J energy and 500-psec duration. (The OFID system has recently[10] been used to generate 30-psec CO_2 laser pulses.) The beam was focused into a cell of hydrogen gas, by spherically corrected germanium lenses of aperture ratio varying from $f/1$ to $f/5$.

The gas was flowed, filtered, and cold-trapped to remove impurities which might cause premature breakdown. For the same reason, it was important to maintain a high peak-to-precursor contrast ratio in the laser pulse.

The electrons were detected by two means: (a) a silicon surface-barrier detector filtered by 3.5 mg/cm^2 of aluminum foil, and (b) Kodak No-Screen medical x-ray film wrapped in a 3.5-mg/cm^2 thickness of Al foil. On the basis of the range-energy relations[11] in the H_2 gas, it was determined that the electrons had an energy of 10–20 keV. This was insufficient to penetrate the aluminum foil. Therefore they were detected indirectly, by means of the bremsstrahlung and Al K x rays produced in the foil.

The film was bent into the shape of a cylinder of 4 cm in diameter, co-axial with the laser beam in the center. Two typical exposures, made with an $f/1$ lens, are shown in Figs. 3(a) and 3(b). The two shots are similar in that the electrons are emitted on either side of the plasma, in the plane formed by the electric vector and the propagation vector. Nevertheless there are shot-to-shot fluctuations and differences. In particular, Fig. 3(b) shows some substructure in the spots which represent the angular distribution of electrons.

As a double check, the plane of optical polarization was rotated by 45° by use of a germanium slab. The shifted spots in Fig. 3(c) show that the directions of electron emission rotated an equivalent amount.

To determine more accurately the direction of electron emission relative to the light wave it was necessary to reduce the angular spread of propagation vectors by using a longer-focal-length lens. With an $f/5$ lens, the spread of k vectors is only $\pm 5°$, and Fig. 4 shows the result. Along the

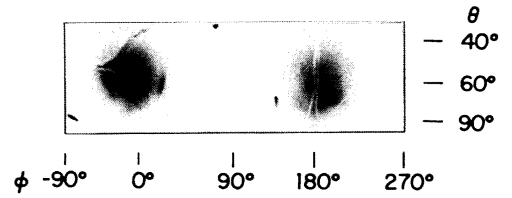

FIG. 4. The exposure due to a plasma produced by an $f/5$ lens. In this case several hundred shots were needed. The thin white lines in the exposed regions are due to wrinkles in the aluminum foil and they should be ignored. θ and φ are spherical coordinates with respect to the propagation and polarization vectors, respectively.

two edges of the film are the azimuthal and polar angles of electron emission with respect to the polarization and propagation vectors, respectively. The electrons were emitted in the plane of optical polarization, but in a direction 30° backward from the electric vector. The half-angle of the two cones of electron emission was about 25°. Therefore no electrons were accelerated into the forward half-sphere, i.e., into the antiparallel directions.

The angle of incidence, θ_m, for maximum electron acceleration is usually given[12] by the following formula which is valid for small θ_m:

$$3kL\sin^3\theta_m = 1, \quad (1)$$

where k is the vacuum propagation constant and L is the density profile scale length. From Fig. 4, $\theta_m = 60°$, which is somewhat too large for formula (1) really to be accurate. Nevertheless, we may conclude that $L \approx 1/2k$ or about 1 μm. Thus the angle of peak fast-electron emission gives us information on the scale length L.

Armed with a knowledge of L, we are able to predict the energy of the fast electrons. A cold-plasma "wave-breaking" analysis[13] is applicable under the physical conditions of our plasma. The "electron overtaking" condition[7] occurs at a kinetic energy $\mathcal{E} = eE_dL$. The evanescent electric field which penetrates to the critical layer, E_d, may be expressed in terms of the free-space electric field, E_0, by using the solution to Maxwell's equations given by Ginzburg[14]:

$$E_d \approx (E_0/2\pi)(\lambda/L)^{1/2}.$$

Therefore, the electrons are ejected from the plasma with an energy

$$\mathcal{E} = eE_0(\lambda L)^{1/2}/2\pi.$$

For a laser intensity of 10^{14} W/cm^2 and $L \sim 1\mu$m (as inferred from θ_m), this yields an electron energy $\mathcal{E} \approx 15$ keV, well within the measured range of energies.

In general, fast electrons are emitted in all outward directions normal to the critical-density surface. Nevertheless, the precise shape of this surface (spherical, ellipsoidal, or irregular) plays only a minor role in the experiments reported here. This is because Eq. (1) selects that angle θ_m along the surface for which the RA effect is maximized. The precise shape of the surface affects mainly the finite spread of angles about the maximum.

It should be kept in mind that the mechanism which produces the plasma density gradient in a gas target is inherently different from that in a solid target. In a gas the density gradient is determined by the propagation mechanism[15] of the ionization front. The motion of the ions themselves is actually quite negligible. In a solid target, on the other hand, the density profile is formed by ablation of ions from the surface. The motion of these ions is strongly influenced by the ponderomotive pressure, and many types of filamentation instabilities[6] are rather probable.

This may explain why gas targets are more suitable for isolating the basic physical processes which occur in laser-plasma interaction. In a solid target there is always something additional taking place, and the simple angular emission described in Fig. 2 has apparently not been observed, though perhaps it soon will be.

More work is needed on the propagation mechanisms[15] of the laser-driven ionization front in a netural gas. The measurement here, of the density profile scale length, $L \sim 1$ μm, is a good starting point. When combined with the avalanche growth rate g of the electron number density, we may deduce[16] a speed of propagation,

$$v = gL.$$

The avalanche ionization scaling laws[17] imply a growth rate $g \approx 10^{12}$ sec^{-1} for H_2 at 150 Torr and 10^{14} W/cm^2. Therefore the calculated propagation speed is $v \approx 10^8$ cm/sec, in good agreement with measurements[5] on the speed[10] of the "plasma shutter."

We acknowledge a valuable discussion with W. L. Kruer.

*Research supported by Advanced Research Projects Agency under Contract No. F44620-75-C-0088.

[1]P. K. Kaw, J. Dawson, W. Kruer, C. Oberman, and E. Valeo, Kvantovaya Elektron. (Moscow) 1, 3 (1971)

[Sov. J. Quantum Electron 1, 205 (1971)].
[2]J. P. Friedberg, R. W. Mitchell, R. L. Morse, and L. I. Rudsinski, Phys. Rev. Lett. 28, 795 (1972).
[3]Eli Yablonovitch, Phys. Rev. Lett. 35, 1346 (1975).
[4]The quiver energy alone is much greater than the ionization potential.
[5]Eli Yablonovitch, Phys. Rev. Lett. 31, 877 (1973).
[6]K. G. Estabrook, E. J. Valeo, and W. L. Kruer, Phys. Fluids 18, 1151 (1975).
[7]J. M. Dawson, Phys. Rev. 113, 382 (1959).
[8]E. Yablonovitch and J. Goldhar, Appl. Phys. Lett. 25, 580 (1974).
[9]H. S. Kwok and E. Yablonovitch, Rev. Sci. Instrum. 46, 814 (1975).
[10]H. S. Kwok and E. Yablonovitch, to be published.
[11]E. Segrè, *Nuclei and Particles* (Benjamin, New York, 1965).
[12]D. V. Giovanielli and R. P. Godwin, Am. J. Phys. 43, 808 (1975).
[13]J. Albritton and P. Koch, Phys. Fluids 18, 1136 (1975).
[14]V. L. Ginzburg, *The Propagation of Electromagnetic Waves in Plasmas* (Pergamon, Oxford, 1970), 2nd ed, see especially Section 20.
[15]Yu. P. Raizer, Usp. Fiz. Nauk 108, 429 (1972) [Sov. Phys. Usp. 15, 688 (1973)].
[16]E. Yablonovitch, to be published.
[17]E. Yablonovitch, Appl. Phys. Lett. 23, 121 (1973).

Radiation-Induced Diffusion of Hydrogen and Deuterium in MgO†

Y. Chen and M. M. Abraham
Solid State Division, Oak Ridge National Laboratory, Oak Ridge, Tennessee 37830

and

H. T. Tohver
University of Alabama, Birmingham, Alabama 35294, and Solid State Division, Oak Ridge National Laboratory, Oak Ridge, Tennessee 37830

(Received 7 September 1976)

We find that the normally stable configuration of substitutional hydrogen and deuterium in MgO becomes highly unstable during ionizing irradiation. The cross section for displacement of hydrogen is found to be a strong function of the irradiating temperature, being $\sim 10^8$ b at 290 K and $\sim 10^6$ b at 85 K. The displacement cross section of hydrogen at 290 K is shown to be twice that of deuterium.

This Letter reports a new phenomenon of exceedingly high diffusivity for substitutional hydrogen and deuterium in MgO under electron irradiation. It establishes that the usual diffusion constants for hydrogen, deuterium, and (by implication) tritium cannot be used to predict the behavior of these isotopes in insulators under irradiation—as for example in thermonuclear applications.

Mass transport of ions in insulating compounds during irradiation has been a much neglected field of study. Little, if any, work has been done in the high-temperature oxides. The lack of activity is due in part to the expected small effects and to the cumbersome measurements required. For hydrogen and deuterium in MgO, however, the latter barrier is partially overcome by infrared spectroscopy, which provides a powerful probe to determine the O-H and O-D stretching modes for several lattice configurations in MgO.

The O-H and O-D stretching frequencies corresponding to several configurations in MgO have been identified in the past.[1-7] In particular, the absorption bands at 3296 and 2445 cm^{-1} have been convincingly attributed to H^+ or D^+, respectively, substituting for Mg^{++} ions. The H^+ or D^+ in this site is affected by covalent bonding to one of the six neighboring oxygen ions and the resultant lattice distortion yields the following configuration: Mg^{2+}-OH^--[Mg vacancy]-O^{2-}-Mg^{2+}. In color-center nomenclature, this defect is referred to as the V_{OH}^- center. Therefore, the amplitudes for the bands at 3296 and 2445 cm^{-1} provide a relative measure of the concentration of the substitutional H^+ and D^+, respectively. Rapid quenching from high temperature (> 1300 K) maximizes the substitutional V_{OH}^- species and minimizes the formation of $Mg(OH)_2$ precipitates, which absorb at 3700 cm^{-1}.[3,6] Slow cooling from elevated temperatures has the reverse effect.

Single crystals from two sources were used. Those from W. & C. Spicer, Ltd., Winchcombe, Gloucestershire, England, contained only hydrogen. The crystals grown in this laboratory were doped with deuterium by soaking the MgO powder in D_2O prior to crystal growth.[8] Because of re-

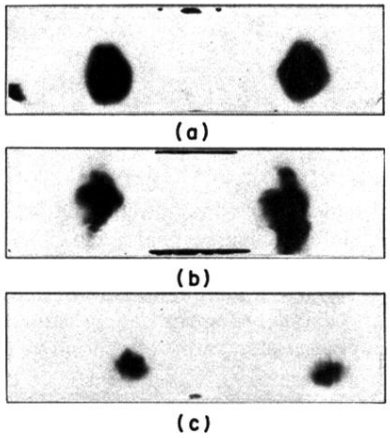

FIG. 3. The x-ray film was bent into the shape of a cylinder, co-axial with the laser beam, and exposed to the fast electrons. (a),(b) two typical shots. Notice the angular substructure in (b). (c) The plane of polarization rotated 45°. The two spots are correspondingly shifted.

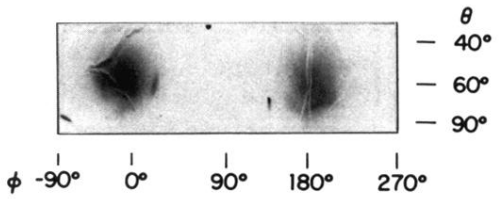

FIG. 4. The exposure due to a plasma produced by an $f/5$ lens. In this case several hundred shots were needed. The thin white lines in the exposed regions are due to wrinkles in the aluminum foil and they should be ignored. θ and φ are spherical coordinates with respect to the propagation and polarization vectors, respectively.